Characteristics of coda envelope for slant-stacked seismogram

Satoshi Matsumoto

Institute of Seismology and Volcanology, Faculty of Sciences, Kyushu University, Shimabara, Japan

Kazusige Obara

National Research Institute for Earth Science and Disaster Prevention, Tsukuba, Japan

Akira Hasegawa

Graduate School of Science, Tohoku University, Sendai, Japan

Abstract. We discuss the single scattering model by using seismic array data. By analyzing observed seismic array records, we found that coda energy level for slant-stacked record is smaller than that for single station record as expected from the single scattering model. The energy level of slant-stacked waveform is dependent on stacking direction. The energy level variation for different slant-stacking directions suggests that horizontally aligned scatterers predominate over vertical ones. The present analysis is probably useful to detect scattering anisotropy.

Introduction

Coda waves have been interpreted as scattered waves by small-scale inhomogeneities randomly distributed within the earth [*Aki*, 1969]. [*Sato* 1977] obtained an analytical solution for the case of single isotropic scattering. Many of studies based on envelope analysis suggest that the single scattering model is applicable to observed coda waves. In seismic array studies, however, no one has discussed the effect of scattered waves from randomly distributed scatterers on the observed envelope. Seismic array can decompose the coda wave into ray direction by stacking. In the present study, we use envelopes of slant-stacked waveforms obtained by a seismic array observation, and discuss about the shape of the envelopes based on the single scattering model.

Single scattering model

Following *Sato* [1977,1982], we briefly describe the single scattering model. For simplicity, we assume that the source radiates energy in spherical symmetry. En-

ergy density $E(r_0, t)$ on a hypocentral distance r_0 at a lapse time t from the origin time can be expressed as follows in a coordinate system shown in Fig. 1.

$$E(r_0, t) = \int \int \int \frac{W_0 g(\psi) K(\theta, \varphi, \theta_0, \varphi_0)}{\beta 4\pi r_1^2 4\pi r_2^2} \times \delta\left(t - \frac{r_1 + r_2}{\beta}\right) d\vec{r}, \qquad (1)$$

where W_0 is radiated energy from the source, β is seismic velocity, $g(\psi)$ is scattering coefficient, and $\vec{r}$ is location vector of scatterer. The formula means that coda energy is obtained by summing up contribution of scattered energy from distributing scatterers in the space as described in *Sato* [1977]. For envelope of slant-stacked waveform by a seismic array, sensitivity of the array varies as a function of both ray direction coming to the array and a direction of slant-stacking. Therefore, we have to take into account a directional weighting function $K(\theta, \varphi, \theta_0, \varphi_0)$ in the kernel of integration, which reflects array response for the case of slant-stack direction in θ_0, φ_0. Transform (1) into prolate-spheroidal coordinate $(x, y, z) \rightarrow (v, w, \varphi)$.

$$E(r_0, t) = H(v - 1)\frac{W_0}{4\pi r_0^2 2\pi} \int_0^{2\pi} d\varphi \int_{-1}^{1} dw \times \frac{g(\psi) K(\theta, \varphi, \theta_0, \varphi_0)}{v^2 - w^2} \qquad (2)$$

$$\cos\theta = \frac{1 + vw}{v + w}, \cos\psi = \frac{2 - v^2 - w^2}{v^2 - w^2},$$

where $H(x)$ is Hevieside step function, v is travel distance normalized by hypocentral distance ($v = \beta t/r_0$). For envelope of single station record, energy is obtained in the case of $K = 1$. For slant-stacked wave, (2) can be rewritten using the angle from the array θ under isotropic scattering hypothesis,
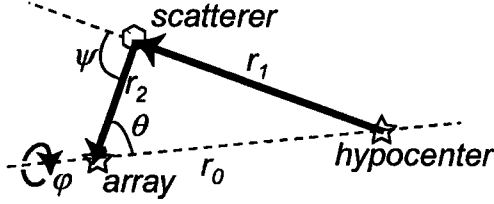
Figure 1. Coordinate system and geometrical relationship among hypocenter, array, and scatterer.

$$E(r_0, t) = H(v-1)\frac{W_0}{4\pi r_0^2 2\pi}\int_0^{2\pi}d\varphi\int_0^{\pi}d\theta$$

$$\times\frac{g_0\sin\theta K(\theta,\varphi,\theta_0,\varphi_0)}{v^2 - 2v\cos\theta + 1}, \quad (3)$$

$$g_0 = \oint g(\psi)d\Omega.$$

For simplicity, we analyze the waveforms in the cases of $\theta_0 = 0$ and π because array response is a function of angle from stacking direction. Namely, we take both direction of hypocenter and the opposite one as the direction of stacking. If the array response has cut-off angle contributing to coda energy from stacking direction, K can be written in a simple form,

$$K(\theta,\varphi) = 1 \quad for \quad \theta_0 \le \theta \le \theta_1$$
$$K(\theta,\varphi) = 0 \quad for \; others$$

In this case, (3) can be integrated analytically as follows.

$$E(r_0, t)$$
$$= H(v-1)\frac{W_0}{4\pi r_0^2}\frac{g_0}{2v}\ln\left|\frac{1 + v^2 - 2v\cos\theta_1}{1 + v^2 - 2v\cos\theta_0}\right|. \quad (4)$$

In the above formula, $\theta_0 = 0, \theta_1 = d\theta$ for stacking the array data into the direction of hypocenter, and $\theta_0 = \pi - d\theta, \theta_1 = \pi$ for the opposite one. For a single station observation, $\theta_0 = 0, \theta_1 = \pi$. By evaluating (4) with $d\theta = \pi/10$, we show in Fig. 2 coda envelopes of waveform at a single station, forward stacking waveform ($\theta_0 = 0$), and backward stacking waveform ($\theta_0 = \pi - d\theta$), respectively. We can see in Fig. 2 that the energy density for the array is smaller than that for the single station. This is attributed to the limiting of the range of integration in (4) for the array data. The energy density for $\theta_0 = 0$ is larger than that for $\theta_0 = \pi - d\theta$. The area on a scattering shell contributing
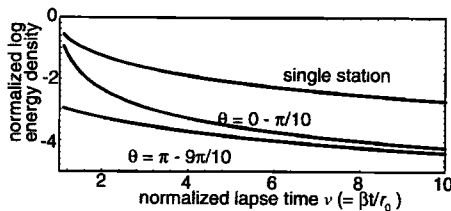

Figure 2. Envelopes calculated from formula (4). The curves show the cases of single station record and slant-stacked ones. The slant-stacking directions face to hypocenter and back to that, respectively.

to coda envelope depends on slant-stacking direction in spite that optic angle from the array is identical. The difference in energy density between $\theta_0 = 0$ and $\theta_0 = \pi$ is the largest among any pair of for θ_0. The difference also depends on hypocentral distance. For larger v, the difference becomes small We have shown the variation of envelopes for slant-stacked waveforms in the above. In the following section, we apply it to the practical case by analyzing waveform data obtained by a seismic array observation in explosion experiments.

Observation

We carried out a seismic array observation in northeastern Japan for the period from Aug. 1 to Nov 12, 1998 [*Matsumoto et al.* 1999]. A mountain chain is running in the middle of the area parallel to the Japan trench. It is formed by horizontally compressional stress field in almost east-west direction. The array is composed of 2Hz vertical and 1Hz 3-component seismometers with a site spacing from 10m to 40m. Vertical and 3-component seismometers were installed at 96 and 32 sites, respectively. The length of the array is about 3km. The location and configuration of the array are shown in Fig. 3. Waveform data from explosions, carried out by Research Group of Explosion Seismology [*Hasegawa and Hirata,* 1999], are recorded by manual triggering.

In the present study, we analyze waveform data from the two explosions whose locations are shown in Fig. 3. Epicentral distances for these shots M2 and M7 are 3.4 and 22.8km, respectively. We apply slant-stack processing to the vertical component of the observed array data from the explosions. Slant-stacked waveforms for the shots are composed of vertical component signals observed at 108 sites with high S/N ratios for both shots. In this study, we use only smoothed coda envelope of slant-stack waveform in order to discuss background (average) scattering strength of inhomogeneity distributed in the whole area. We assume that scattered waves coming from the stacking direction are incoherent.
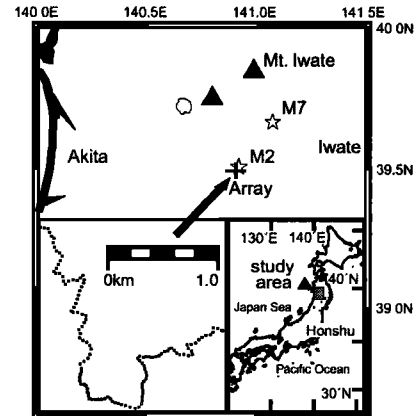

Figure 3. Map showing locations of seismic array and two explosions. Stars show shot points of explosions M2 and M7 in 1998. Cross symbol denotes location of the active volcanoes. Array profile is shown in the lower left, solid squares being observation sites.
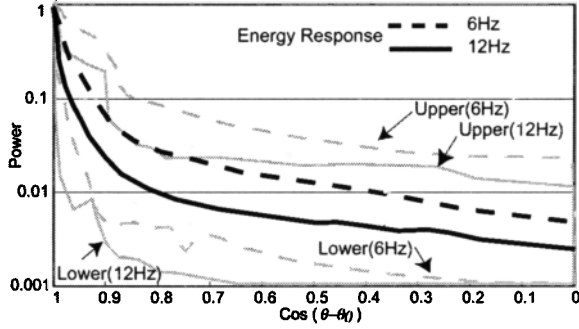
Figure 4. Energy response estimated from slant-stacked waveforms for various ray direction (θ, φ) in fixed stacking direction (θ_0, φ_0). Solid and dashed lines are average value of those for 6 and 12Hz ranges, respectively. Gray lines show higher and lower limits of distributing range of the values.

In order to evaluate formula (4), we check the response of the array for various ray directions. For a certain ray direction, seismograms of waves propagating to the direction are synthesized for seismometers of the array. To obtain the seismogram at a site, sinusoidal wave with one cycle is assigned to time series with a time shift calculated from site location and assumed ray direction. Synthetic seismograms are calculated every 0.01 s/km between -0.2 and 0.2s/km in both north-south and east-west direction. After slant-stacking the synthetic array seismograms for a ray direction (θ, φ) in a given stacking direction (θ_0, φ_0), energy response is obtained from squared stacked wave amplitude. The distribution of energy response is estimated from the above mentioned calculation for various ray directions (θ, φ), which is plotted against $\cos(\theta - \theta_0)$ in Fig. 4. The array response check is carried out for two frequency bands of 6 and 12Hz. Generally speaking, the decay of the response against the angle between stacking and ray directions becomes stronger with increasing frequency. Contributions of energy from out of stacking direction amount to 1/10 of that from stacking direction, when the discrepancy between ray and stacking directions is larger than about $\pi/10 (= \cos^{-1}(0.8))$. In this study, we only discuss first order approximation for simplicity. Therefore, we adopt $\pi/10$ as cut-off angle $\delta\theta$ in (4).

Envelope of slant-stacked waveform

First, we discuss envelope shape for both single station and array data. Figure 5 shows band-pass filtered envelopes of 4–8Hz (center is 6Hz), and of 8–16Hz (center is 12Hz) both for shorter (M2) and longer distance explosions (M7). Gray line shows envelope observed at one station among the array. Solid and dashed lines are obtained from slant-stacked waveforms in the direction of hypocenter and in the opposite direction (0 and 180 °), respectively. Each envelope is obtained by taking root means square amplitude of filtered seismogram with a moving time window of 0.5 seconds. The single station envelope and those for the array are nor-

malized by direct P wave amplitudes. There is a clear difference in energy level between the single and the array envelopes. In stacked envelopes, the energy level depends on the stacking direction. Especially, it is remarkable for the longer distance shot at lower frequency. Thick solid lines are expected coda envelopes for single and stacked envelopes, which are calculated from (4) with an exponential dumping factor. In (4), attenuation effect due to propagation in the medium is not considered. Therefore, we need to add an alternative exponential dumping factor to (4) in order to apply to the practical case. The applied attenuation factors to the envelopes in the figure are determined to match the observed ones for every shot and frequency. For each shot and frequency band, contribution of the factor to the envelope is identical with one another at same lapse time since the factor is independent of integration range in (4). The observed envelopes agree with theoretically expected ones in the longer distance shot. This result suggests that energy contribution from scattering shell is what the single scattering model predicts and that the single scattering model is applicable to the observed records. This means scatterer distributes homogeneously in the region. For the shorter distance shot, observed amplitude in the later part for 0°is slightly larger than that for 180°as theoretically predicted. In the earlier part of envelope, the theoretically expected envelope for 180°is smaller than the observed one. Perhaps this is caused by the assumption of the array response having a boxcar shape with $\pi/10$ cut-off angle. The direct P wave amplitude and the following larger amplitude appeared in direct P wave direction leak to the envelope slant-stacked in the direction of 180°.

According to (4), the envelope of slant-stacked wave is independent of φ because area on scattering shell contributing to coda wave is the same for any φ in the case of incidence to the array with fixed θ. However, if scatterers have the orientation like cracks often discussed in the studies about velocity anisotropy, then the envelope with the same θ is dependent on φ. Here, we discuss di-
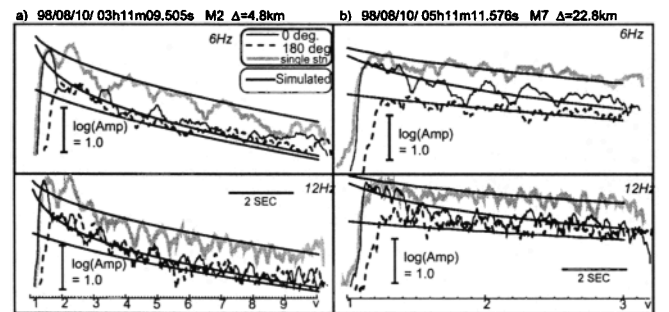

Figure 5. Envelopes observed and theoretically expected for 6 and 12 Hz ranges. a) and b) are those for epicentral distance of 4.8 and 22.8km, respectively. Gray lines are envelopes of the single station record. Solid and dashed lines are slant-stacked envelopes in the direction of 0 and 180°. Thick solid lines are theoretical curves of the single isotropic scattering model.
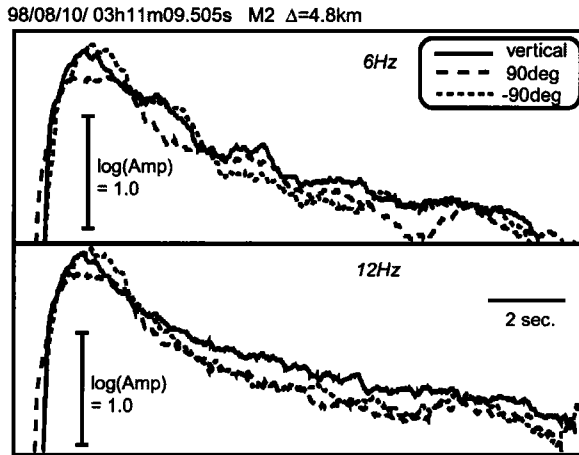
98/08/10/ 03h11m09.505s M2 Δ=4.8km

Figure 6. Envelopes of three stacked waveforms from shot M2 for 6 and 12Hz ranges. The envelopes show the cases of vertical incidence (solid line), 90°(dashed) and -90°(dotted).

rective domination of scattering strength. Records from the shorter distance explosion are analyzed, since effective orientation of scatterer is varied with lapse time for slant-stacked waveform in a certain fixed ray direction. However, for short distance explosion, the effective orientation of scatterer is constant for fixed θ. To keep constant θ, we select and fix azimuth of 90°from that of direct P wave as slant-stacking azimuth. Slownesses adopted here to slant-stack are -0.19, 0.19, and 0 s/km. These values mean that three ray directions coming to the array are restricted in 90°clockwise and counterclockwise from direct P wave direction, and in vertical. If scattering property of the medium has anisotropy, it is expected that coda energy level is different from each other among these envelopes. Figure 6 shows envelopes of three stacked waveforms for 6 and 12Hz with a smoothing window length of 1 second for stabilizing envelope shape. The envelopes of vertical incidence (solid line) to the array have slightly higher level than the other envelopes for both frequency ranges. In addition, the same feature can be seen for other shots with short hypocentral distances. This means that vertical reflection is stronger than horizontal reflection. Scattering angle is almost backward because of small epicentral distance, which implies that backward scattering coefficient is dependent on vertical angle to the scatterer distributing in this area. As the simplest model, we suppose that horizontal reflectors are dominant to vertical ones. The area sampled by scattered waves is the crust for the lapse time range presently analyzed. For lower frequency, the difference of coda level between vertical and horizontal one is smaller than that for higher frequency. This is probablly due to effect of frequency dependence of scattering anisotropy that becomes isotropic for lower frequency. As mentioned above, the crust in northeastern Japan is under horizon-

tally compressional stress field probably caused by the subduction of the Pacific Plate. Fluids such as magma or water intruded are expected to spread horizontally under this compressional stress field. We estimate that this causes the scattering coefficient in the crust of this region predominant in the vertical direction.

Conclusions

We analyzed envelopes of slant-stacked waveforms based on the single scattering model. Then availability of the single scattering model is confirmed based on the difference between envelopes stacked in the direction of hypocenter and the opposite one. It is estimated that horizontally aligned scatterers predominate to vertical ones from the stacked wave analysis in the 90°from direct wave direction. The present method is probably effective for detecting scattering anisotropy.

References

Aki, K., Analysis of the seismic coda of local earthquakes as scattered waves, *J. Geophys. Res.*, *74*, 615-631, 1969.

Hasegawa, A., and N. Hirata, Northeastern Japan Transect - deformation process of the crust and crustal activity in the island arc (in Japanese), *Chikyu*, *27*,5-11, 1999.

Matsumoto, S., K. Obara, K. Yoshimoto, T. Saito, A. Hasegawa, and A. Ito, Imaging of inhomogeneous structure of the crust beneath Ou Backbone Range, northeastern Japan, based on small aperture seismic array observation (in Japanese with English abstract), *Zisin*, *2*, 52, 283-297, 1999.

Sato, H., Energy propagation including scattering effects: single isotropic scattering approximation, *J. Phys. Earth*, *25*, 27-41, 1977.

Sato, H., Coda wave excitation due to nonisotropic scattering and nonspherical source radiation, *J. Geophys. Res.*, *87*, 8665-8674, 1982.

S. Matsumoto, Institute of Seismology and Volcanology, Faculty of Sciences, Kyushu University, Shimabara 855-0843, Japan. (e-mail: matumoto@sevo.kyushu-u.ac.jp)

K. Obara, National Research Institute for Earth Science and Disaster Prevention, Tsukuba 305-0006, Japan. (e-mail: obara@bosai.go.jp)

A. Hasegawa, Research Center for Prediction of Earthquakes and Volcanic Eruptions, Graduate School of Science, Tohoku University, Sendai 980-8578, Japan. (e-mail: hasegawa@aob.geophys.tohoku.ac.jp)